High-quality strain-relaxed SiGe films grown with low temperature Si buffer

Y. H. Luo,[a] J. Wan, R. L. Forrest,[b] J. L. Liu, M. S. Goorsky,[b] and K. L. Wang
Device Research Laboratory, Department of Electrical Engineering,
University of California at Los Angeles, Los Angeles, California 90095-1594

(Received 5 February 2001; accepted for publication 2 April 2001)

High-quality strain-relaxed SiGe templates with a low threading dislocation density and smooth surface are critical for device performance. In this work, SiGe films on low temperature Si buffer layers were grown by solid-source molecular beam epitaxy and characterized by atomic force microscope, double-axis x-ray diffraction, photoluminescence spectroscopy, and Raman spectroscopy. Effects of the growth temperature and the thickness of the low temperature Si buffer were studied. It was demonstrated that when using proper growth conditions for the low temperature Si buffer the Si buffer became tensily strained and gave rise to the compliant effect. The lattice mismatch between the SiGe and the Si buffer layer was reduced. A 500 nm $Si_{0.7}Ge_{0.3}$ film with a low threading dislocation density as well as smooth surface was obtained by this method. © *2001 American Institute of Physics.* [DOI: 10.1063/1.1375801]

I. INTRODUCTION

High-quality strain-relaxed SiGe buffer layers, which are used as ''virtual substrates'' for growth of strain Si/SiGe high electron mobility transistors, metal–oxide–semiconductor field effect transistors[1,2] and Ge photodiodes on Si,[3] have attracted considerable attention for their device applications. However, the large lattice mismatch (~4.17%) between Si and Ge usually results in a high density of misfit dislocations at the interface of SiGe and Si, and lots of threading dislocations propagating through the SiGe buffer layer into the active layers. The threading dislocations deteriorate the device performance.[4,5] Several methods have been used to grow high quality strain-relaxed SiGe films, such as graded composition,[6] compliant substrate,[7] and growth on patterned substrate,[8] etc. Recent reports indicated that the use of low temperature (LT) buffer layers could significantly reduce the threading dislocation density in the SiGe layer.[9,10] It was believed that the LT Si layer not only provides low energy sites for dislocation nucleation, or point defects for trapping of propagating dislocations, but also involves in strain adjustment.[11] In this work, LT Si buffer layers were used to grow high-quality strain-relaxed SiGe films and the mechanism of this method was studied by using atomic force microscopy (AFM), high resolution double-axis x-ray diffraction (DAXRD), photoluminescence (PL), and Raman spectroscopy. Using the LT Si buffer, a 500 nm $Si_{0.7}Ge_{0.3}$ film with low threading dislocation density and smooth surface was obtained and characterized by AFM and an etch-pit-density (EPD) method.

II. EXPERIMENT

The samples investigated were grown by solid source molecular beam epitaxy (MBE) in a Perkin–Elmer system. A P^- type Si (001) substrate was cleaned using a modified Shiraki method and loaded into the MBE system after a diluted HF dip. At first, a 60 nm Si buffer was grown at 600 °C to reduce the defects and smooth the surface of the substrate. A followed-up LT Si layer was grown at a temperature range from 300 to 420 °C. Then a SiGe layer was grown on the top of the LT Si buffer at 480 °C. The growth rate for both the Si layer and the SiGe layer was about 1 Å/s. LT Si buffers were grown at different growth temperatures and with various thicknesses.

The surface morphology and microroughness of the samples were characterized by using a Park Scientific AFM in a contact mode. The surface roughness was evaluated by the root mean square (rms) of the AFM profile. The alloy composition and degree of strain relaxation were determined from DAXRD. Low temperature PL was measured at 4.5 K using an Ar^+ 488 nm laser line. Raman spectroscopy was used to measure the strain and estimate the quality of the SiGe layer. Raman spectroscopy has been proven to be sensitive to strain and dislocations in semiconductor heterostructures as a contactless probing technique.[12,13] In this work, Raman spectra were taken using a 457.9 nm Ar^+ laser line with a microscope entrance, giving a 0.7 μm laser spot on the sample.

III. RESULTS AND DISCUSSION

A. Influence of the LT Si buffer growth temperature

150 nm $Si_{0.8}Ge_{0.2}$ samples were grown on 200 nm LT Si buffer layers, which were previously grown at different temperatures. Figure 1 shows the rms surface roughness measured by the AFM. The 400 °C was found to be the optimum temperature to achieve the smoothest surface and ordered crosshatches on the surface.

The Raman spectra were shown in Fig. 2(a), showing Si–Si peaks from the SiGe layer and the Si substrate. By using an iterated Lorentzian fit to the curves, the peak position and full width at half maximum (FWHM) were ob-

[a]Electronic mail: yuhao@ee.ucla.edu
[b]Also at: Department of Materials Science and Engineering, University of California at Los Angeles, Los Angeles, CA 90095.

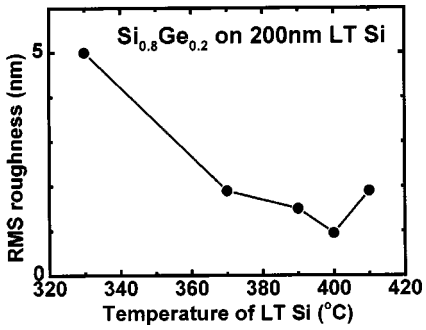

FIG. 1. AFM rms surface roughness of the 150 nm $Si_{0.8}Ge_{0.2}$ film on a 200 nm LT Si buffer vs the growth temperature of the LT Si buffer. 400 °C was found to be the optimum growth temperature for the LT Si buffer layer.

tained. The position and the FWHM of the Si–Si peak from the SiGe layer with different temperature buffers are shown in Fig. 2(b). Compared with Fig. 1, the trend of the FWHM matches that of the rms roughness result from AFM while the trend of the peak position is just the reverse of the rms roughness. It is known that the stress only shifts the peak without changing the FWHM of the peak while threading dislocations and defects make the Si–Si peak redshifted and wider.[12,13] The peak position and FWHM of the Raman results implied that the defect density of the sample with a 400 °C LT Si buffer was the lowest. The sample with the 410 °C LT Si buffer was just a little rougher as observed by AFM. However, the Raman peak redshifted substantially and the FWHM was much larger, indicating that there was a high density of defects. For the sample with a 390 °C LT Si buffer, though no ordered crosshatches were observed, since

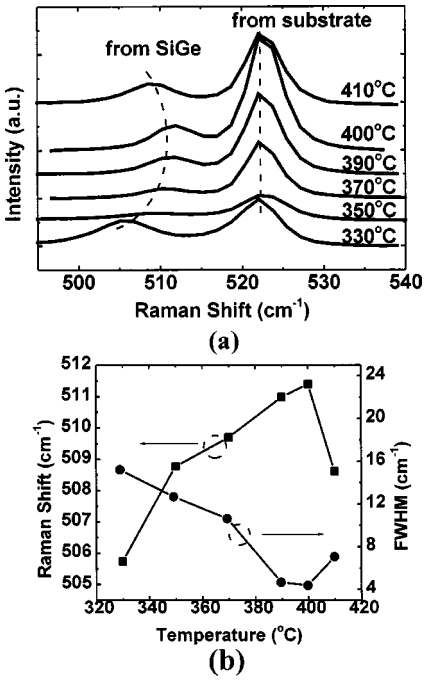

FIG. 2. (a) Raman spectra of the 150 nm $Si_{0.8}Ge_{0.2}$ samples on the LT Si buffer grown at different temperatures. Two peaks correspond to the Si–Si peak (~510 cm^{-1}) from the SiGe layer, the Si buffer and substrate (~522 cm^{-1}), respectively. (b) Peak position and FWHM of the Si–Si peak of the SiGe layers versus the growth temperature of the LT Si buffer.

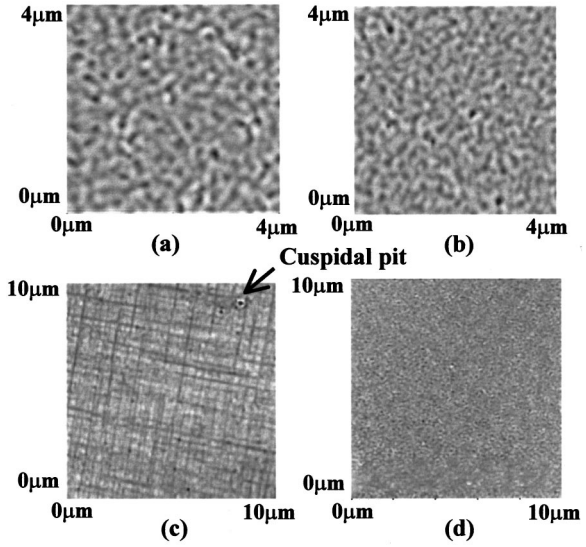

FIG. 3. AFM surface morphology of a 200 nm $Si_{0.8}Ge_{0.2}$ film grown on a 400 °C LT Si buffer with thickness (a) 50, (b) 100, (c) 200, and (d) 250 nm. Crosshatches and cuspidal pits are clearly observed in (c).

the Raman shift and FWHM was very close to that of the sample with a 400 °C buffer, the crystalline quality was believed to be quite closed to that of the 400 °C sample. For samples with a LT Si buffer grown at a temperature around 400 °C the quality of the SiGe layer was the best, while for too low and too high temperatures the quality deteriorated. As a reference, another sample was grown at 480 °C for both the SiGe layer and the Si buffer. The surface roughness was 1.9 nm, somewhat larger than that of the 410 °C sample. The peak position and the FWHM of Si–Si peak from the SiGe layer in the Raman spectra were 510.5 and 6.3 cm^{-1}, respectively.

For temperatures around 400 °C for the LT Si layer, it was believed that the high concentration point defects, which were generated during the low temperature growth, provided nucleation centers for the formation of misfit dislocations and decreased the density of threading dislocations in the SiGe layer. For higher growth temperatures, the point defect density in the LT Si buffer was too low to release the mismatch effectively. For lower growth temperatures, although many point defects were generated, they may aggregate and form stacking faults even before the deposition of the SiGe.

B. Influence of the thickness of the LT Si buffer layer

It is well known that the surface morphology and the roughness of epitaxial layers are influenced by misfit and threading dislocations.[14,15] Figure 3 shows the AFM images of the samples with different thicknesses of the LT Si buffer layers. The rms surface roughness is shown in Fig. 4 as a function of LT Si buffer thickness. The roughness decreased linearly from 14 to 1 nm with the LT Si thickness varying from 50 to 200 nm, then increased slightly from 1 to 2 nm when the thickness increased to 300 nm. Threading dislocations generated from the interface of the LT Si and SiGe caused surface undulation. For the 200 nm sample, ordered and straight crosshatch lines were observed on the surface, as

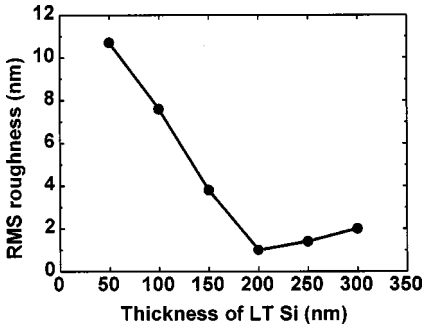

FIG. 4. AFM rms surface roughness of the 200 nm $Si_{0.8}Ge_{0.2}$ films vs the LT Si thickness grown at 400 °C. The optimum thickness for the LT Si buffer layer was found to be 200 nm.

shown in Fig. 3(c). There were also some cuspidal pits on the surface. The crosshatch pattern on the surface was due to misfit dislocations traveling at the Si/SiGe interface[14] and each misfit dislocation was normally associated with two threading dislocations. The cuspidal pits observed on the surface of the samples shown arose from the local stress field of threading dislocations.[15] The threading dislocation density was equal to the density of the cuspidal pits on surface ($\sim 10^7\ cm^{-2}$); the threading dislocation density was the lowest for sample with the 200 nm buffer. For other samples with thinner LT Si buffers, the surface was much rougher and no ordered crosshatches were observed. The huge x-ray ω-full width at half-maximum (FWHM) for these samples shown later (Fig. 5) indicated that they had a high mosaic spread, probably due to a high density of dislocations and/or

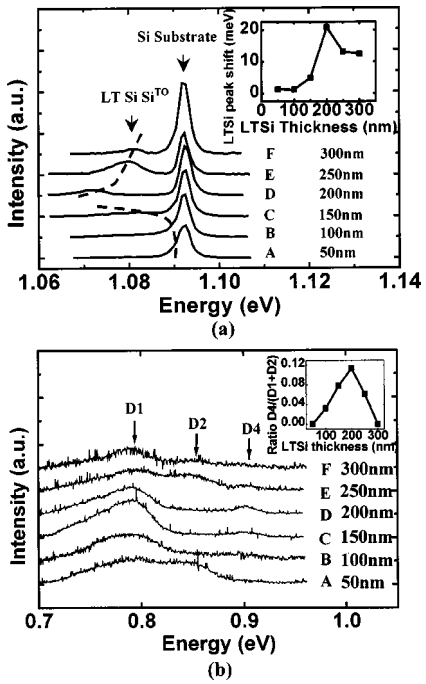

FIG. 5. (a) High energy parts of PL spectra from samples A through F. The peak to the left of the Si TO peak of the substrate came from the LT Si buffer layer. The inset shows the shift value of the left peak (TO of LT Si) with respect to the substrate Si TO peak. (b) Low energy parts of PL spectra from sample A through F. The peaks are labeled as D1, D2, and D4 dislocation lines, respectively. The inset shows the integrated intensity ratio of the D4 peak to the D1 and D2 peak D4/(D1+D2).

three dimensional growth (=roughness). The density of misfit dislocations may be too high to be observed with AFM. For the samples having buffers thicker than 200 nm [Fig. 3(d)], the surface was just a little rougher, but there was no clear crosshatch observed on the surface. In this case, the point defect density in the LT Si layer was maybe so high that some of them annihilated and formed stacking faults before the deposition of the SiGe layer began.

Table I gives the results for samples measured by DAXRD to confirm the composition, relaxation, and crystal quality. The strain relaxation was determined by employing a high-resolution x-ray reciprocal space mapping technique, which allows a direct elucidation of the strain status of the epilayer via a (224) reciprocal space map, independent of the composition of the SiGe layer. The composition was then determined from a scan of the (004) peak using the measured relaxation. It was found that too thin a LT Si buffer (50–100 nm) leads to a fully relaxed SiGe layer with a very poor crystalline quality (ω-FWHM$\sim$3500 arc sec). The SiGe peak from sample D with a 200 nm LT Si buffer had the smallest ω-FWHM among all the samples (ω-FWHM $=1000$ arc sec), indicating the lowest misfit dislocation density, in agreement with the roughness data. The SiGe layer from sample D was determined to be 62% relaxed.

In Fig. 5(a), the high-energy parts of PL spectra from the samples are shown. For samples A and B, a shoulder to the left of the strong Si transverse optical (TO) peak from the substrate was observed (as indicated by dash lines). For samples C, D, E, and F, the peak became stronger and separated from the major Si TO peak. Using a Gaussian fit to these two peaks, the positions of the peaks were determined. The TO Si peak from the Si substrate remains at 1.092 eV, while the left peak changed position with the thickness of the LT Si buffer layer. The inset in Fig. 5(a) shows the shift of the left peak with respect to the Si TO peak as a function of the thickness of the LT Si buffer. At first (A–C), the redshift of the peak increases with the thickness of LT Si buffer layer, reaching a maximum value for the 200 nm LT Si buffer sample (D), then decreases slowly (E–F). It is believed that this peak is the Si TO peak from the LT Si buffer and the tensile strain of the LT Si buffer causes the redshift. The maximum redshift for sample D indicates the highest tensile strain of the LT Si buffer, consistent with DAXRD result as discussed above. From the relationship between the energy band gap change and strain of the strain Si on $Si_{1-x}Ge_x E_g(Si)-0.4$,[16] the strain may be estimated from the

TABLE I. The Ge composition, strain relaxation, and SiGe peak ω-FWHM determined from DAXRD measurements for 200 nm SiGe films on different thick LT Si buffer layers. The sample number is indicated in the parentheses.

LT Si thickness (nm)	Ge (x)	SiGe relaxation (%)	FWHM of SiGe (004) peak (arc sec)
50 (A)	0.16 ± 0.01	100 ± 20	3500 ± 500
100 (B)	0.17 ± 0.01	100 ± 20	3500 ± 500
200 (D)	0.18 ± 0.005	62 ± 3	1000 ± 50
250 (E)	0.18 ± 0.01	53 ± 8	1100 ± 50
300 (F)	0.19 ± 0.005	68 ± 8	1400 ± 50

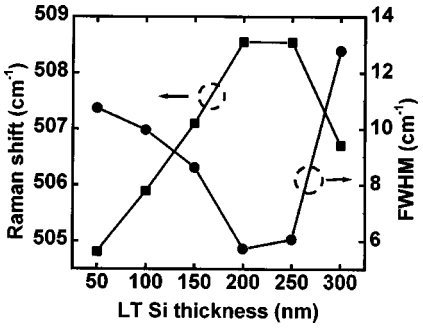

FIG. 6. Peak position and FWHM of the Si–Si peak from the SiGe layers vs the thickness of the LT Si buffer for 200 nm $Si_{0.8}Ge_{0.2}$ on a LT Si buffer grown at 400 °C.

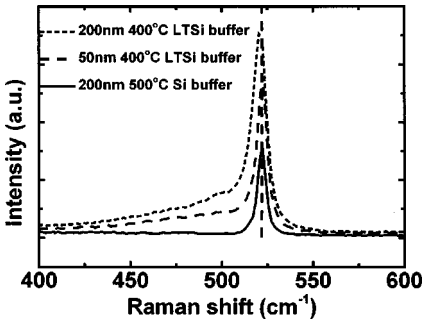

FIG. 7. Raman spectra from Si buffer layers. From top to bottom: 200 nm 400 °C LT Si buffer layer, 50 nm 400 °C LT Si buffer layer, and 200 nm 500 °C LT Si buffer layer. The dash straight line indicates the peak position of the unstrained Si–Si line.

redshift. For sample D, the shift of 20 meV corresponds to the strain Si on $Si_{0.95}Ge_{0.05}$. Since the Ge composition of the SiGe layer on LT Si layer is about 0.18, the strain of the LT Si layer is about 28% of the fully mismatched strain between the Si and the $Si_{0.82}Ge_{0.18}$. Because of this accommodation the misfit dislocation density decreased.

The low energy parts of PL spectra are shown in Fig. 5(b). For clarity, the PL intensities are not to scale. A peak (D4) at about 0.9 eV was observed for samples B, C, D, and E, but did not show up in samples A and F. This peak was attributed to the D4 dislocation line. The threading dislocations in the SiGe layers, the Si buffer and substrate, and extended straight segments of misfit dislocations are responsible for the D4 dislocation line.[17,18] Since the SiGe layer in our samples was only 200 nm thick, the straight segments of misfit dislocations and threading dislocations in the LT Si buffer and the Si substrate were the dominating source of the D4 line. The D1 and D2 lines were from the dislocation intersections.[17,18] The integrated intensity ratio of D4/(D1+D2) is shown in the inset of Fig. 6(b). The highest D4/(D1+D2) intensity ratio in sample D implies that the misfit dislocations are longest with the lest intersections and/or the density of threading dislocations confined in LT Si buffer and Si substrate is the highest. Both cases indicated the lowest threading dislocation density in the SiGe layer.

The same series of samples were measured by Raman spectroscopy for the strain relaxation and film quality. The peak position and the FWHM of the Si–Si peak of the SiGe layer with different thicknesses of buffers are shown in Fig. 6. Similar to the analysis in Sec. A, the Raman results also implied that the defect density of the sample with a 200 nm LT Si buffer was the lowest. For the sample with a 250 nm LT Si buffer, even though no ordered crosshatch was observed, as indicated the Raman shift and FWHM, the threading dislocation density of this sample and the crystal quality was quite close to the 200 nm LT Si sample. This result was also confirmed by the x-ray analysis. The sample with 300 nm LT Si buffer was just little rougher. However, the Raman peak redshifted substantially and the FWHM was much larger. This indicated a high density of defects.

The Raman spectra for a 50 nm and a 200 nm 400 °C LT Si buffer samples without a SiGe layer are shown in Fig. 7. For comparison, the spectrum for a 200 nm Si buffer layer grown at 500 °C is also shown. For the 50 nm LT Si buffer, there was a tail to the left side of the Si–Si peak of the LT Si buffers coming from the point defects in the LT Si layer. However, for the 200 nm LT Si buffer, in addition to a larger tail to the left, the Si–Si peak redshifted about 1.5 cm^{-1} and the FWHM was much larger than that of the 50 nm LT Si buffer. The later two facts were attributed to the disorder and point defects in the LT Si buffer. This indicated that the 200 nm LT Si buffer had a much higher density of point defects than the 50 nm LT Si buffer, and these point defects worked to improve the quality of the SiGe layer.

C. Thick SiGe film

A 500 nm $Si_{0.7}Ge_{0.3}$ film was grown by using a 200 nm 400 °C LT Si buffer for observing further improvement of threading dislocation density in the SiGe layer. The rms surface roughness was measured by AFM to be 1.9 nm. The etch pits of the sample was revealed by using an Schimmel defect selective etch and imaged by a Nomarski microscope. From the EPD shown in Fig. 8, the threading dislocation density was estimated as 1.5×10^5 cm^{-2}.

IV. CONCLUSION

In conclusion, the compliant substrate effect of the low temperature Si buffer layer for growth of high quality thin relaxed SiGe layers was demonstrated. The influences of the growth temperature and the thickness of the LT Si buffer on

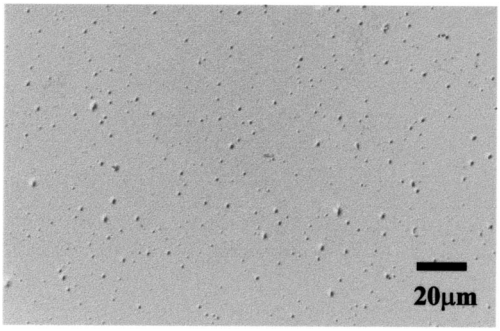

FIG. 8. Nomarski image of the 500 nm $Si_{0.7}Ge_{0.3}$ film on a 200 nm 400 °C LT Si buffer after Schimmel defect selective etch, showing the etch pits which arise from the threading dislocations. The threading dislocation density is estimated as 1.5×10^5 cm^{-2}.

the quality of the SiGe layer were studied using AFM, DAXRD, PL, and Raman measurements. It was shown that the LT Si buffer became tensily strained and the lattice mismatch between the buffer layer and the SiGe layer was reduced. The high concentration point defects, which were generated during the low temperature growth, provided nucleation centers for the formation of misfit dislocations and decreased the density of threading dislocations in the SiGe layer. These kinds of films are being qualified for the fabrication of heterojunction bipolar transistors.

ACKNOWLEDGMENTS

The work was supported by Semiconductor Research Corporation and UCMICRO-Conexant.

[1] K. Ismail, F. K. LeGoues, K. L. Saenger, M. Arafa, J. O. Chu, P. M. Mooney, and B. S. Meyerson, Phys. Rev. Lett. **73**, 3447 (1994).
[2] Y. H. Xie, D. Monroe, E. A. Fitzgerald, P. J. Silverman, F. A. Theil, and G. P. Watson, Appl. Phys. Lett. **63**, 2263 (1993).
[3] L. Colace, G. Masini, G. Assanto, H.-C. Luan, K. Wada, and L. C. Kimerling, Appl. Phys. Lett. **76**, 1231 (2000).
[4] R. Hull, J. C. Bean, and C. Buescher, J. Appl. Phys. **66**, 5837 (1989).
[5] L. B. Freund, J. Appl. Phys. **68**, 2073 (1990).
[6] J. L. Liu, C. D. Moore, G. D. U'Ren, Y. H. Luo, Y. Lu, G. Jin, S. G. Thomas, M. S. Goorsky, and K. L. Wang, Appl. Phys. Lett. **75**, 1586 (1999).
[7] Y. H. Luo, J. L. Liu, G. Jin, K. L. Wang, C. D. Moore, M. A. Goorsky, C. Chih, and K. N. Tu, J. Electron. Mater. **29**, 950 (2000).
[8] A. Nishida, K. Nakagawa, E. Murakami, and M. Miyao, J. Appl. Phys. **71**, 5913 (1992).
[9] H. Chen, L. W. Guo, Q. Cui, Q. Hu, Q. Huang, and J. M. Zhou, J. Appl. Phys. **79**, 1167 (1996).
[10] P. M. Mooney, J. L. Jordan-Sweet, K. Ismail, J. O. Chu, R. M. Feenstra, and F. K. LeGoues, Appl. Phys. Lett. **67**, 2373 (1995).
[11] Y. H. Luo, J. Wan, R. L. Forrest, J. L. Liu, G. Jin, M. S. Goorsky, and K. L. Wang, Appl. Phys. Lett. **78**, 454 (2001).
[12] J. Takahashi and T. Makino, J. Appl. Phys. **63**, 87 (1988).
[13] D. J. Olego, H. Baumgart, and C. K. Celler, Appl. Phys. Lett. **52**, 483 (1988).
[14] E. A. Stach, K. W. Schwarz, R. Hull, F. M. Ross, and R. M. Tromp, Phys. Rev. Lett. **84**, 947 (2000).
[15] J. W. P. Hsu, E. A. Fitzgerald, Y. H. Xie, P. J. Silverman, and M. J. Cardillo, Appl. Phys. Lett. **61**, 1293 (1992).
[16] G. Abstreiter, H. Brugger, T. Wolf, H. Jorke, and H. J. Herzog, Phys. Rev. Lett. **54**, 2441 (1985).
[17] H. P. Tang, L. Vescan, C. Dieker, K. Schmidt, H. Luth, and H. D. Li, J. Cryst. Growth **125**, 301 (1992).
[18] E. A. Steinman, V. I. Vdovin, T. G. Yuhova, V. S. Avrutin, and N. F. Izyumskaya, Semicond. Sci. Technol. **14**, 582 (1999).